Combined Microdialysis-Tumor Homogenate Method for the Study of the Steady State Compartmental Distribution of a Hydrophobic Anticancer Drug in Patient-Derived Xenografts

Carles Monterrubio, Sonia Paco, Monica Vila-Ubach, Eva Rodríguez, Romina Glisoni, Cinzia Lavarino, Paula Schaiquevich, et al.

Volume 32 | Number 4 | April 2015

PHARMACEU... RESEARCH

aaps An Official Journal of the American Association of Pharmaceutical Scientists

ONLINE FIRST

Springer

11095 | ISSN 0724-8741
32(4) 1161-1518 (2015)

Springer

Springer

RESEARCH PAPER

Combined Microdialysis-Tumor Homogenate Method for the Study of the Steady State Compartmental Distribution of a Hydrophobic Anticancer Drug in Patient-Derived Xenografts

Carles Monterrubio • Sonia Paco • Monica Vila-Ubach • Eva Rodríguez • Romina Glisoni • Cinzia Lavarino • Paula Schaiquevich • Alejandro Sosnik • Jaume Mora • Angel M. Carcaboso

ABSTRACT

Purpose To develop a reproducible microdialysis-tumor homogenate method for the study of the intratumor distribution of a highly hydrophobic anticancer drug (SN-38; 7-ethyl-10-hydroxycamptothecin) in neuroblastoma patient-derived xenografts. **Methods** We studied the nonspecific binding of SN-38 to the microdialysis tubing in the presence of 2-hydroxypropyl-beta-cyclodextrin (HPBCD) in the perfusate. We calibrated the microdialysis probes by the zero flow rate (ZFR) method and calculated the enhancement factor (f = extrapolated SN-38 concentration at the ZFR / SN-38 concentration in the dialysed solution) of HPBCD. We characterized the extravasation of HPBCD to tumors engrafted in mice. *In vivo* microdialysis and terminal homogenate data at the steady state (subcutaneous pump infusions) were used to calculate the volume of distribution of unbound SN-38 ($V_{u,tumor}$) in neuroblastoma. **Results** HPBCD (10% *w/v*) in the perfusate prevented the nonspecific binding of SN-38 to the microdialysis probe and enhanced SN-38 recovery (f = 1.86). The extravasation of HPBCD in the tumor during microdialysis was lower than 1%. $V_{u,tumor}$ values were above 3 mL/g tumor for both neuroblastoma models and suggested efficient cellular penetration of SN-38.

Conclusions The method contributes to overcome the limitations of the microdialysis technique in hydrophobic drugs and provides a powerful tool to characterize compartmental anticancer drug distribution in xenografts.

ABBREVIATIONS

ECF	Extracellular fluid
ER	Enhanced recovery
f	Enhancement factor
FEP	Fluorinated ethylene propylene
HPBCD	2-hydroxypropyl-beta-cyclodextrin
PDX	Patient-derived xenograft
RR	Relative recovery
SN-38 C	SN-38 Carboxylate
SN-38 L	SN-38 Lactone
tECF	Tumor extracellular fluid
ZFR	Zero flow rate

C. Monterrubio · S. Paco · M. Vila-Ubach · E. Rodríguez · C. Lavarino · J. Mora · A. M. Carcaboso
Department of Pediatric Hematology and Oncology,
Hospital Sant Joan de Déu Barcelona,
Esplugues de Llobregat, Spain

C. Monterrubio · S. Paco · M. Vila-Ubach · E. Rodríguez · C. Lavarino · J. Mora · A. M. Carcaboso (✉)
Preclinical Therapeutics and Drug Delivery Research Program,
Developmental Tumor Biology Laboratory,
Fundació Sant Joan de Déu, Santa Rosa, 39-57,
Esplugues de Llobregat, Barcelona, Spain
e-mail: amontero@fsjd.org

R. Glisoni
CONICET-Department of Pharmaceutical Technology, Faculty of Pharmacy and Biochemistry, Universidad de Buenos Aires, Buenos Aires, Argentina

P. Schaiquevich
CONICET-Clinical Pharmacokinetics Unit, Hospital de Pediatria JP Garrahan, Buenos Aires, Argentina

A. Sosnik
Department of Materials Science and Engineering, Technion-Israel Institute of Technology, Haifa, Israel

Springer

INTRODUCTION

Many potentially active anticancer agents are poorly distributed in tumors or display excessive systemic toxicity at concentrations required to achieve their pharmacological effect at the tumor cell level (1, 2). Thus, optimization of chemotherapeutic drug delivery to the solid tumor microenvironment has become one of the most studied fields in cancer research (3). Drug penetration of solid tumors might be improved by concomitant treatments targeting biological and physical properties of the tumor stroma (4), active transport at the tumor cells (5), or *via* new drug delivery systems (6). All these approaches require an accurate evaluation of the pursued pharmacokinetic effects, *i.e.*, accumulation of the drug in the tumor cell to increase therapeutic efficacy and, ideally, low systemic exposure to reduce side effects. Such pharmacokinetic evaluation may be achieved by measuring the amount of drug in the tumor by methods involving drug administration to preclinical models (usually mice), blood sampling at different time points and terminal collection of tumor tissue. This approach requires a large number of animals to provide a complete concentration-time profile of drug distribution in the tumor (7). The simplicity of the analysis of tumor homogenates is an advantage of this method. However, this –the traditional– approach does not provide information regarding drug distribution in the solid tumor compartments (extracellular, intracellular and vascular). Such information is relevant to understand drug activity (or lack thereof) and pharmacokinetic interactions. For instance, if the amount of drug detected in the homogenate is predominantly accumulated in the extracellular fluid of tumor (tECF), suitable intracellular drug targets might not be reached (7).

The combination of two different sampling methods, microdialysis and tumor homogenates, under steady state drug pharmacokinetics helps to accurately determine drug distribution in solid tumors using a low number of experimental animals. Microdialysis is used to sample the tECF for the subsequent analysis of levels of free (protein unbound) compounds, in equilibrium with the free compound in plasma (8). Then, the ratio at the steady state between the total drug concentration in the tumor homogenate and the unbound drug concentration in the tECF (calculated by microdialysis) provides the unbound drug volume of distribution in tumor ($V_{u,tumor}$), measured in mL/g tumor (9), as calculated from Eq. 1

$$V_{u,tumor} = \frac{A_{tot,\,tumor} - V_{tot,\,blood} \times C_{tot,\,blood}}{C_{ss,tumor}} \quad (1)$$

where $A_{tot,tumor}$ is the total amount of drug per gram of tumor homogenate (including tumor blood), $V_{tot,blood}$ is the volume of blood per gram of tumor, $C_{tot,blood}$ is the total concentration of drug in blood, and $C_{ss,tumor}$ is the concentration of unbound

drug in the tECF at the steady state. High values of the $V_{u,tumor}$ parameter indicate high distribution of the drug in the intracellular compartment of the tumor or nonspecifically bound to tumor tissue components, whereas low values suggest that the drug is predominantly distributed in the extracellular space.

The steady state approach in animals with microdialysis probes allows the determination of real-time effects of concomitant treatments on the compartmental distribution of the assayed chemotherapeutic drug. Steady state intratumor microdialysis in combination with terminal tumor sampling (homogenates) was utilized for the first time to study the shift in the distribution toward the cellular compartment of the water-soluble drug topotecan in brain tumors upon the effect of efflux pump inhibition at the tumor cell level (10). However, the application of the microdialysis technique to highly hydrophobic anticancer drugs has remained elusive, due to the lack of reproducibility of the conventional microdialysis principle in compounds that bind nonspecifically to parts of the microdialysis device (internal surface of tubing and probe membrane) and other plastic or glass surfaces used during the posterior analysis (11–13). For instance, previous studies on the microdialysis of the anticancer drugs docetaxel and doxorubicin have resulted in low or erratic probe recovery due to nonspecific binding (11, 12). To overcome such problem some authors propose the addition of solubilizers to the perfusate, such as 2-hydroxypropyl-beta-cyclodextrin (HPBCD) (14, 15), proteins to block the nonspecific binding sites in the circuit (16), or chemical agents with affinity to the collected molecule (17), while others have applied mathematical approaches to eliminate the binding component from the microdialysis recovery value (13, 18).

The objective of this study was to develop a reproducible method for the assessment of the tumor pharmacokinetics of the highly hydrophobic anticancer drug SN-38 (7-ethyl-10-hydroxycamptothecin) in mice bearing patient-derived xenografts (PDX) of the pediatric solid tumor neuroblastoma. SN-38 is a potent topoisomerase I inhibitor that results from the hydrolysis of irinotecan, its soluble prodrug. Two forms of SN-38 are in equilibrium in water, the active lactone (SN-38 L) and the non-active hydrophilic carboxylate (SN-38 C). SN-38 L predominates under acidic pH conditions, whereas SN-38 C at neutral and basic pH. Here, we propose a steady state microdialysis-homogenate method to study the intratumor distribution of SN-38 L without the interference of SN-38 C.

MATERIALS AND METHODS

Reagents

SN-38 was obtained from Seqchem (Pangbourne, UK). Irinotecan for *in vivo* studies was purchased from Hospira

(Lake City, IL). Phosphate buffered saline (PBS) tablets, HPBCD (molecular weight of 1400 g/mol), collagenase IV, fluorescein isothiocyanate (FITC), *N,N*-dimethylformamide (DMF) and dimethyl sulfoxide (DMSO) were purchased from Sigma-Aldrich (St. Louis, MO). Triethylamine (TEA), glacial acetic acid, sodium phosphate monobasic monohydrate and di-sodium tetra-borate 10-hydrate were from Panreac (Barcelona, Spain), and acetonitrile and methanol from Merck (Darmstad, Germany).

Tumor Models

Two patient-derived neuroblastoma animal models were used: HSJD-NB-003 and HSDJ-NB-004. Both models have been produced from patient biopsies obtained at Hospital Sant Joan de Déu (HSJD) (Barcelona, Spain) from patients at diagnosis as part of an IRB-approved protocol. Additional information of both models is available in Suppl. Material. Fresh tumor fragments were transplanted to the flank of athymic nude mice (Harlan, Indianapolis, IN) to establish xenografts models. The research performed with mice adhered to the Principles of Laboratory Animal Care (NIH publication #85-23, revised in 1985).

SN-38 Analysis by High Performance Liquid Chromatography (HPLC)

The analytical technique was slightly modified from the one described by Warner and Burke (19). A stock solution of SN-38 (1 mg/mL in DMSO, stored at −80°C) was used to prepare standards (STDs) and quality controls (QCs) for analysis of SN-38 in dialysates, mouse plasma, mouse blood and tumor homogenates, prepared as previously described (10). The stock solution was first diluted in methanol to obtain an intermediate concentration of 0.02 mg/mL of SN-38. This solution was further diluted either in methanol (working solutions for SN-38 L) or di-sodium tetra-borate 10-hydrate 0.04 N in water (working solutions for SN-38 C) to achieve concentrations of 50, 100, 200, 500, 1000 and 2000 ng/mL (to prepare STDs) and 150 and 1500 ng/mL (to prepare QCs). Working solutions for SN-38 C were kept at room temperature for 45 min protected from light to achieve total conversion from lactone to carboxylate. Then, each working solution (5 µL) of each SN-38 concentration was added to PBS, 10% HPBCD in PBS (*w/v*), mouse plasma (Janvier, Saint Berthevin Cedex, France), mouse blood or tumor homogenate (490 µL) to build the STDs (final concentrations of 0.5, 1, 2, 5, 10, 20 ng/mL) and QCs (final concentrations of 1.5 and 15 ng/mL). The solution was then vortexed and quickly added (200 µL) to cold methanol (800 µL) to avoid the pH-dependent interconversion between SN-38 C and SN-38 L. Mouse plasma required centrifugation (2 min, 10,000 rpm) to separate methanol-precipitated plasma proteins before injection of the

supernatant to the HPLC system (10 µL). Tumor homogenates and mouse blood required centrifugation (2 min, 10, 000 rpm) and filtration of the supernatant through 0.45 µm pore membrane CA Spin-X centrifuge tube filters (Costar, Cambridge, MA) before injection in the HPLC.

The HPLC system (Shimadzu, Kyoto, Japan) consisted of a pump model LC-20 AD, an autosampler module SIL-20 AC XR and a fluorescence detector RF-20A XS set at 379 nm and 560 nm for excitation and emission wavelengths. The mobile phase consisted of a pH 5.5 TE-acetate buffer (3% TE in water, *v/v*) and acetonitrile (74:26) and the column was a Tracer Excel 120 ODSA C18 (150 mm×4.6 mm, 5 µm) (Teknokroma, Barcelona, Spain).

Binding to Tubing

We studied whether increasing amounts of HPBCD in the perfusate would prevent nonspecific adsorption of SN-38 (L and C) to the plastic tubing of the microdialysis circuit. In a preliminary experiment, we determined the time to achieve the equilibrium between SN-38 L and SN-38 C (defined as less than 1% of SN-38 L-to-SN-38 C conversion in a period of 1 h) at pH 7.4 at room temperature by sequential sampling and HPLC analysis of a 20 ng/mL SN-38 L solution prepared in PBS. Then, 20 ng/mL SN-38 L solutions were prepared in PBS and allowed to reach the lactone-carboxylate equilibrium for the time determined. HPBCD in different proportions (0, 2, 4, 6, 8 and 10%*w/v*) was added to the equilibrated SN-38 solution. The solutions were then loaded into syringes and perfused with a pump (Kd Scientific KDS-101-CE, Holliston, MA) at a flow rate of 0.5 µL/min through polyurethane (0.35 mm internal diameter, donated by Raumedic, Voiron, France) and fluorinated ethylene propylene tubes (FEP, 0.13 mm internal diameter, Idex Health and Science, Oak Harbor, WA). The length of the tubes was selected to provide a total internal surface of 100 mm^2. Then, samples were collected every 20 min in glass sealed vials containing 40 µL methanol (methanol stops the interconversion of both SN-38 forms upon storage) placed in a CMA 470 refrigerated fraction collector (CMA, Kista, Sweden), at 6°C. Samples were stored at −80°C until HPLC analysis. Tube binding was defined as the absolute change in the concentration of the perfused solution during perfusion through the tube and calculated according to Eq. 2

$$\text{Binding } (\%) = \left| 1 - \frac{C_{rec}}{C_{per}} \right| \times 100 \tag{2}$$

where C_{rec} is the concentration of SN-38 recovered after perfusion through the tube and C_{per} is the concentration of SN-38 in the perfused solution.

We applied the one-sample *t*-test to compare mean tube binding values to a hypothetical zero value using Graphpad Prism 5 software (La Jolla, CA).

SN-38 Microdialysis: Enhanced Relative Recovery and Repeatability

Since the addition of HPBCD to the perfusate has been shown to enhance the relative recovery of hydrophobic drugs by microdialysis (14, 20, 21), we expected a similar result for SN-38, and more specifically for its hydrophobic and active form SN-38 L. Thus, we performed an experiment to address such enhancing effect. We used the CMA 20 microdialysis probe with a membrane length of 4 mm and 20 kDa molecular weight cutoff (CMA, Kista, Sweden), in a microdialysis circuit composed of a pump, a swivel (Instech 375/D/22QM; Plymouth Meeting, PA), a 25 cm length FEP tube and a CMA 470 refrigerated sample collector.

For enhanced relative recovery experiments, a clinically relevant 20 ng/mL SN-38 solution was prepared in PBS pH 7.4 and placed in a glass light-protected beaker, and stirred at room temperature overnight for equilibration between SN-38 L and SN-38 C. The next day, 10% HPBCD in PBS was perfused through the probe at 0.5 μL/min. An identical experiment was run in parallel using PBS alone (no HPBCD) as perfusate. Dialysate samples were collected over 20 min intervals for a total of 7 sampling periods and the relative recovery (RR) assessed according to Eq. 3

$$RR\ (\%) = \frac{C_{dial}}{C_0} \times 100 \tag{3}$$

where C_{dial} is the concentration of SN-38 in the dialysates and C_0 is the concentration of SN-38 in the dialysed solution.

To address the repeatability of the enhanced recovery, following the relative recovery experiment the probe was transferred to SN-38-free PBS for 7 sampling periods and finally returne to the original 20 ng/mL SN-38 to collect 6 more sampling periods. Sealed glass vials with 40 μL of cold methanol were used to collect the samples.

To further study the enhancing effect of the cyclodextrin additive on the microdialysis relative recovery, a third experiment was performed under the same conditions; the SN-38 20 ng/mL solution was prepared in 10% HPBCD in PBS and dialyzed with a 10% HPBCD solution perfused at 0.5 μL/min.

Probe Calibration by the Zero Flow Rate Method (ZFR)

The predicted enhancing effect of HPBCD on the relative recovery of SN-38 is likely due to the formation of the inclusion complex between the drug and HPBCD in the probe

lumen that drives additional mass transport of the drug towards the dialysate (21). Thus, the retrodialysis method or the use of internal standard in the perfusate were excluded to calculate the probe recovery *in vivo*. Alternatively, the most suitable method to calibrate the probe *in vivo* was the ZFR, which takes advantage of (i) the constant tECF concentration of the analyte at steady state plasma drug levels and (ii) the exponential relationship between relative recovery and flow rate through the probe (22). A set of experiments was performed *in vitro* to calculate the relative recovery by the ZFR method, in which SN-38 (20 ng/mL concentrations prepared in PBS and kept overnight to equilibrate SN-38 L and SN-38 C) was dialyzed with a CMA 20 probe perfused with 10% HPBCD in PBS at 0.5, 1, 1.5 and 2 μL/min flow rates. Dialysates were allowed to stabilize for at least twice the time required to wash the dead volume of the circuit after changing flow rates (80, 40, 30 and 20 min for 0.5, 1, 1.5 and 2 μL/min respectively). The exponential ZFR curve was extrapolated by nonlinear regression to fit the data using the following Eq. 4

$$C_{dial} = C_{ZFR} \times e^{(-KF)} \tag{4}$$

where C_{dial} is the concentration of SN-38 in dialysate samples at flow rate F, C_{ZFR} is the concentration of SN-38 calculated by nonlinear regression at the zero flow rate value, and K is a constant defined by the product of the mass transport coefficient and the surface area of the probe membrane, as previously described (23). Under enhancement conditions (*i.e.*, presence of 10% HPBCD as enhancer in the dialysate), the value calculated for C_{ZFR} is higher than C_0 and their relationship is defined by the enhancement factor (*f*) of the recovery, according to Eq. 5

$$f = \frac{C_{ZFR}}{C_0} \tag{5}$$

where C_0 and C_{ZFR} have been defined in Eqs. 3 and 4, respectively. Thus, the enhanced recovery (ER) at a given flow rate, when C_0 is unknown (*e.g.*, upon *in vivo* conditions), is the dialysate concentration at such flow rate divided by C_{ZFR} and multiplied by *f*, as expressed in Eq. 6

$$ER\ (\%) = \frac{C_{dial}}{C_{ZFR}} \times f \times 100 \tag{6}$$

As an intermediate step between *in vitro* and *in vivo* assays, SN-38 microdialyses were performed using a suspension of digested tumor tissue as dialysis solution, stirred and maintained at 37°C during the experiments. Briefly, 1 g of tumor freshly excised from a mouse was digested with collagenase IV

(Sigma) for 1 h in a Thermomixer® shaking incubator (Eppendorf, Hamburg, Germany) set at 37°C and 1300 rpm. The digested tissue was filtered through a 40 µm pore cell strainer, centrifuged at 400 g and the pellet was resuspended with PBS (1 g tumor/1 mL PBS). A solution of SN-38 (10 µg/mL in methanol) was added to the suspension of digested tumor for a final concentration of 20 ng/mL SN-38. Once in equilibrium, a ZFR experiment was performed keeping the solution at 37°C and 300 rpm in the shaking incubator. Samples were collected and stored as detailed above.

Extravasation of HPBCD during Microdialysis

Because dialysates contain 10% HPBCD, we expected that a fraction of the enhancer would be transferred to the dialyzed sample or tissue during the microdialysis experiment. To study such effect *in vitro*, we labeled HPBCD with FITC by reacting 300 mg of cyclodextrin and 83 mg of the tracer in 5 mL of DMF at 32°C for 12 h protected from light. The product (HPBCD-FITC) was then dissolved 10% w/v in PBS and perfused at a flow rate of 0.5 µL/min through a CMA 20 probe immersed in a blank PBS solution. Perfusate, dialysate and blank solution were analyzed for HPBCD-FITC with a ND-1000 nanodrop spectrophotometer (Thermo Scientific, Waltham, MA) at 495 nm.

For *in vivo* studies, 10% HPBCD-FITC in PBS was perfused at 0.5 µL/min through CMA 20 microdialysis probes inserted in subcutaneous tumors (HSJD-NB-003) grown in the flank of athymic nude mice ($n=3$) in accordance with the institutional ethics committee for animal welfare. Perfusate and dialysate samples were analyzed after 2 h collection by spectrophotometry. At the end of the experiment, mice were anesthetized and perfused with PBS and formalin. Then the probe was removed, the tumor excised and cut frozen to study the distribution of HPBCD-FITC surrounding the probe by microscopy (Leica DM 5000 B, Wetzlar, Germany).

Blood Volume in Tumors

To calculate the fraction of blood volume in the tumor we counted the number of erythrocytes in blood and tumor (HSJD-NB-003 and HSJD-NB-004) in athymic nude mice ($n=4$ and $n=3$, respectively) using an Advia 2120 hematology analyzer (Siemens, Erlangen, Germany). Briefly, blood samples were obtained by retroorbital plexus and diluted with PBS prior to analysis. Then mice were euthanized and tumors (15 mm diameter) excised, weighed and digested with collagenase IV at a concentration of 100 mg tumor per mL of collagenase IV (1 h, 1300 rpm, 37°C). After digestion the cell suspension was filtered through a 40 µm pore nylon filter (Teknokroma), 5 mL PBS were added and the mixture

centrifuged for 10 min at 400 g. The supernatant was removed and the pellet was resuspended in 5 mL PBS, filtered and centrifuged again. The pellet was finally resuspended in PBS for a final concentration of 100 mg tumor/mL and the number of erythrocytes quantified. From the erythrocyte counts in blood and tumor, we calculated the volume of blood (% v/w) in tumor tissue.

Plasma Protein Binding

To calculate the unbound fraction of SN-38 in plasma we used the ultrafiltration method (Centrifree Ultrafiltration Device with Ultracel YM-T membrane, Merk Millipore, Billerica, MA). Briefly, 150 µL samples of 200 ng/mL SN-38 in equilibrium in mouse plasma were ultrafiltrated in triplicate. The difference of concentration between the initial sample (bound and unbound SN-38, C_0) and the filtrated sample (free drug, C_f) was equivalent to the SN-38 protein binding (PB), as detailed in Eq. 7

$$PB\ (\%) = \frac{C_0 - C_f}{C_0} \times 100 \qquad (7)$$

SN-38 Steady State Pharmacokinetics after Irinotecan Infusion

To achieve steady state concentrations of unbound SN-38 L in plasma ($C_{ss,plasma}$) and tECF ($C_{ss,tumor}$) we loaded the prodrug irinotecan in osmotic pumps (model 2001D, Alzet, Cupertino, CA) and implanted them subcutaneously in athymic nude mice. We performed a preliminary pharmacokinetic study to characterize the steady state concentrations of unbound SN-38 L achieved for 24 h, in which 19 mice received a dose of 130 µg/h irinotecan and were bled (50 µL) by the retroorbital plexus at times 1, 2, 3, 6, 16 and 24 h (maximum of 3 blood samples per mouse) after pump implantation. Samples were processed for HPLC analysis and data were fitted with ADAPT 5 software (BMSR, Los Angeles, CA) (24).

Combined Microdialysis-Tumor Homogenate Method

To produce subcutaneous solid tumors in nude mice (4 week old females), one fragment of viable tumor tissue (5–10 mm³ of HSJD-NB-003 and HSJD-NB-004 models) was implanted in one flank under isoflurane anesthesia. When the tumor reached 15 mm diameter (7–8 weeks after insertion) a microdialysis experiment was performed in $n=3$ and $n=4$ mice, respectively. First, a CMA 20 probe was inserted in the tumor under isoflurane anesthesia. After probe equilibration (90 min at 0.5 µL/min; 10% HPBCD in PBS), an irinotecan-loaded osmotic pump (130 µg/h) was inserted subcutaneously in the

opposite flank under isoflurane anesthesia. Dialysates were collected overnight every 90 min, into glass sealed vials pre-filled with 180 μL methanol in the refrigerated automatic fraction collector at 6°C. Mice remained awake and freely moving during sample collection. The next day (16–19 h after pump insertion), a blood sample was collected to determine the steady state concentration of SN-38 L in plasma ($C_{ss,plasma}$) and blood ($C_{tot,blood}$). Then, taking advantage of the steady state concentrations of SN-38 L in tECF, the ZFR method was performed during the last 3 h of the *in vivo* experiment, to calculate the recovery (ER) of the probe as detailed in Eq. 6. Thus, the real steady-state concentration of SN-38 L in tECF ($C_{ss,tumor}$) was calculated according to Eq. 8

$$C_{ss,tumor} = \frac{C_{dial}}{ER(\%)} \times 100 \qquad (8)$$

where C_{dial} is the concentration in tumor dialysates (mean of 3 samples in steady state equilibrium). The steady state drug penetration of tECF (P_{tumor}) by unbound SN-38 L was calculated according to Eq. 9

$$P_{tumor} = \frac{C_{ss,tumor}}{C_{ss,plasma}} \qquad (9)$$

After the microdialysis experiment mice were euthanized and the tumor terminally collected to process as homogenate. To calculate the $V_{u,tumor}$ parameter as defined in Eq. 1, homogenates and blood samples were terminally obtained from additional $n=8$ (HSJD-NB-003) and $n=8$ (HSJD-NB-004) mice at 16–19 h after the implantation of the pump. The tumor was weighed, mechanically minced and 10 μL of distilled water was added per mg of tumor. The mixture was sonicated with a Vibracell VCX 750 (Sonics, Newtown, CT) and processed for HPLC analysis.

RESULTS

HPLC Technique

Retention times of SN-38 C and SN-38 L were 7 and 10 min, respectively, and they were not altered by the presence of HPBCD in the samples. The lowest limit of quantification was 0.5 ng/mL for SN-38 L and SN-38 C in PBS, PBS with 10% HPBCD, plasma and blood and 5 ng/g for SN-38 L and SN-38 C in tumor homogenates. No carryover was detected upon the injection of analytical blanks. STDs and QCs were stable at −80°C for at least 2 months.

Binding to Tubing

Because SN-38 L undergoes conversion predominantly to SN-38 C in PBS at pH 7.4, we studied the time required to achieve the equilibrium between both forms in this medium at room temperature (Fig. 1). The conversion rate followed first-order kinetics. After 11 h, SN-38 C and SN-38 L were in equilibrium, with a final molar ratio of 7:93 (SN-38 L:SN-38 C) with a standard deviation of ±0.4%. Such equilibrated solution was used to study the binding of each SN-38 form to both tubing types. Results are shown in Fig. 2. The first observation was that in the absence of HPBCD SN-38 binds tightly and erratically to tubing (28–72%), regardless of its kind. The addition of increasing amounts of HPBCD reduced the binding until the values were not distinguishable from the 0% value observed with 10% HPBCD (one-sample *t*-test; $P=0.960$).

SN-38 Microdialysis

In vitro microdialysis experiments mimicked materials and dead volumes of the tubing and connections (*i.e.* swivel, CMA 20 probe, FEP tube and cannula for septa of the fraction collector) employed further for *in vivo* experiments. As shown in Fig. 3a, the recovery of SN-38 L and SN-38 C was neither enhanced nor repeatable when the perfusate solution was plain PBS. Carryover of SN-38 L persisted during several sampling periods after the probe was transferred to SN-38-free PBS. In contrast, the addition of 10% HPBCD to the perfusate enhanced RR up to 129.6±8.1% for SN-38 L and 71.9±8.9% for SN-38 C (Fig. 3b). There was no quantifiable SN-38 after 3 washing periods (60 min total) in SN-38-free PBS, corresponding to 1.8 times the dead volume (17 μL) of the system.

The enhancing effect of HPBCD was abolished, as expected, by the addition of the same compound (10% HPBCD) to the perfused SN-38 solution. Under this condition, RR for SN-38 L and SN-38 C were 23.9±1.2 and 18.2±0.7%, respectively, and remained constant during the experiment.

Probe Calibration by the ZFR Method

The ZFR method was performed at the end of each *in vitro* experiment to determine RR of SN-38 C and SN-38 L. Data from the ZFR experiments could be fitted to exponential curves by nonlinear regression. For experiments in PBS, R^2 values were 0.969±0.02 and 0.974±0.025 for SN-38 C and SN-38 L, respectively ($n=8$) (Fig. 4a). For experiments with tumor disaggregate suspensions, R^2 was 0.979±0.027 and 0.986±0.003 for SN-38 C and SN-38 L respectively ($n=3$) (Fig. 4b).

At 0.5 μL/min flow rate, the calculated recovery by the ZFR method was 70.8±4.9 and 70.3±7.8% for SN-38 L and

Fig. 1 Kinetics of the conversion of SN-38 L (*red bar*) to SN-38 C (*blue bar*) in PBS pH 7.4 at 20°C. At t = 0 h SN-38 L was 100%; equilibrium was achieved after 11 h of conversion with a final proportion of 7:93 (SN-38 L:SN-38 C).
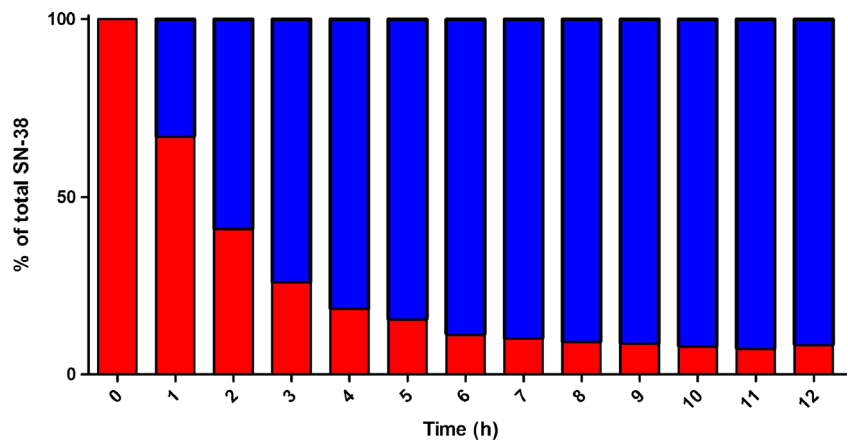
SN-38 C in PBS solution, respectively. Slightly lower values of 56.6 ± 6.7 and $64.3 \pm 3.8\%$ were obtained for the lactone and the carboxylate in disaggregated tumor suspension. The *f* of SN-38 L in PBS was 1.94 ± 0.18. As expected, the RR of the hydrophilic SN-38 C was not significantly enhanced by HPBCD ($f = 1.07 \pm 0.20$). When using disaggregated tumor as dialysis solution, *f* was 1.86 ± 0.26 and 1.13 ± 0.24 for SN-38 L and SN-38 C, respectively. Thus, *f* values in PBS solutions and stirred tumor suspensions matched well. The mean *f* value for SN-38 L obtained from experiments with SN-38 in digested tumor was consequently used to calculate the ER *in vivo* by the ZFR method.

Extravasation of HPBCD during Microdialysis

In vitro, 99.2% of the perfused HPBCD-FITC was recovered in the dialysate and 0.8% was delivered to the perfusate. *In vivo*, the recovered fraction of HPBCD-FITC was $100.2 \pm 2.8\%$. The tumor in contact with the probe track in the HPBCD-FITC perfused tumors presented a microscopic histology similar to the tumor distant to the probe (Fig. 5a and b). The extravasation of the fluorescent HPBCD could be detected by microscopy at a distance of 1.6 mm surrounding the probe track (Fig. 5c).

Plasma Protein Binding and Blood Volume in Tumors

The ultrafiltrated fraction of SN-38 L was $18.6 \pm 2.1\%$. Thus, 81.4% of SN-38 L was bound to plasma proteins. Blood volume in tumors determined by the hematology analyzer was 26.5 ± 5.4 µL/g tumor and 15.4 ± 4.5 µL/g tumor for HSJD-NB-003 and HSJD-NB-004, respectively ($n = 3$).

### Pharmacokinetics of SN-38 Infusions

We evaluated the steady state concentration of SN-38 L in plasma samples obtained from 19 mice infused with irinotecan-loaded pumps at a rate of 130 µg irinotecan/h. The mean plasma concentration of unbound SN-38 L achieved after 16–24 h of infusion was 6.6 ± 1.9 ng/mL (Fig. 6).

Combined Microdialysis-Tumor Homogenate Method

The microdialysis-tumor homogenate experiment focused on the determination of SN-38 L in tumor dialysates, blood and tumor homogenates upon the administration of irinotecan by infusion. The enhancement factor ($f = 1.86$) determined in disaggregated tumors *in vitro* was used to calculate the enhanced

Fig. 2 Binding of SN-38 C and SN-38 L to FEP (**a**) and polyurethane (**b**) tubing perfused with and equilibrated SN-38 solution (20 ng/mL) in 0, 2, 6 and 10% HPBCD in PBS.
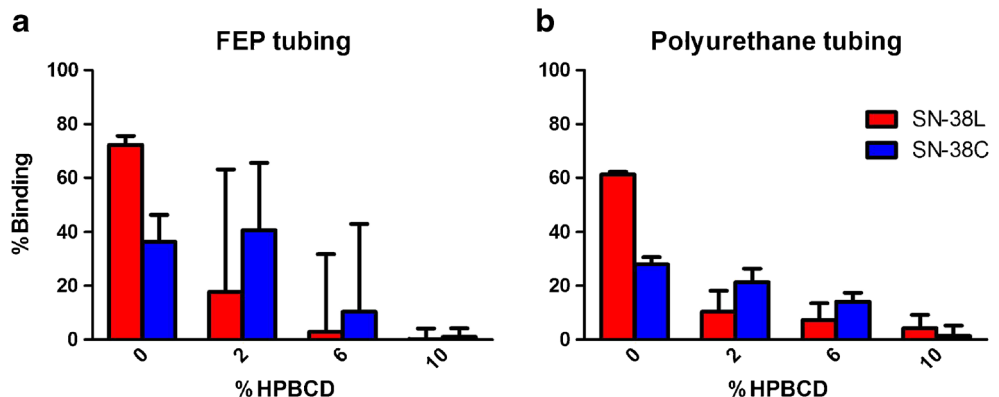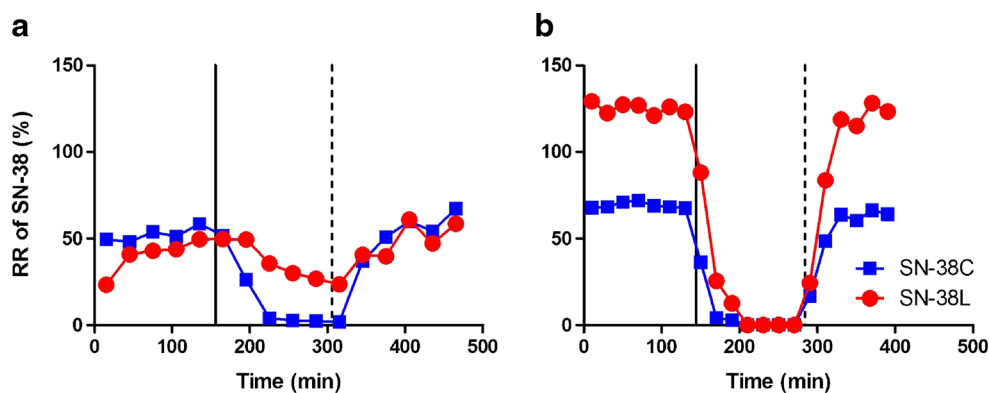
Fig. 3 Relative recoveries of SN-38 C and SN-38 L using plain PBS (HPBCD-free) (**a**) and PBS 10% HPBCD (*w/v*) (**b**) perfusates. *Solid lines* indicate the time when the microdialysis probe was transferred from the dialysis solution containing SN-38 to a plain PBS solution. *Dashed lines* indicate the time when the microdialysis probe was transferred from the plain PBS solution to the dialysis solution containing SN-38.

recoveries of the microdialysis experiments. After *in vivo* microdialysis experiments, ER values for SN-38 L were 132.2± 23.7% and 130.4±25.9% for HSJD-NB-003 (*n*=3) and HSJD-NB-004 (*n*=4), respectively. These data were used to estimate the real concentration in tECF according to Eq. 8 (Fig. 7). Additionally, terminal homogenates and blood samples collected from additional mice infused with irinotecan were analyzed. Results of the whole set of experiments are shown in Table I.

DISCUSSION

Preclinical intratumor distribution of anticancer drugs is accurately addressed by specific sampling and analysis methods combining microdialysis and tumor homogenates (10). However, the application of microdialysis to lipophilic agents in a reproducible and controlled (calibrated) way *in vivo* has remained an unmet challenge (11, 25). Here, we describe a new method for the accurate determination of the distribution parameter $V_{u,tumor}$ of the highly hydrophobic agent SN-38 in patient derived solid tumor xenografts, using HPBCD-enhanced microdialysis under steady-state pharmacokinetics.

We provide a way to calibrate the probe *in vivo*, based on the application of an enhancement factor-corrected ZFR method.

The microdialysis method proposed here is based on the addition of HPBCD as enhancer to the perfusate, as previously described for other drugs (21, 26). HPBCD was more effective than lipids (27) and polymeric surfactant (own experiments; data not shown). Cyclodextrins are cyclic oligosaccharides used in the pharmaceutical field to increment the apparent solubility and stability of compounds (28, 29). We demonstrated that without the addition of at least 10% HPBCD to the dialysate, drug recovery was erratic and low, as reported for doxorubicin and docetaxel elsewhere (11, 12). Our experimental design proved that, in the presence of 10% HPBCD in the perfusate, changes in concentration of the dialysate were not due to tubing uptake and washout. As expected, we found that the recovery of the hydrophilic SN-38 C compound in equilibrium with the hydrophobic SN-38 L was not enhanced by HPBCD, which is a direct evidence that HPBCD enhances only the recovery of hydrophobic compounds due to the formation of inclusion complexes (30). Our experimental observations contrast with previous reports using enhancer-free microdialysis for *in vivo* sampling of SN-38 (31, 32). However, such reports did not provide experimental

Fig. 4 Nonlinear regression analysis of data obtained from ZFR experiments using a dialysis solution consisting of SN-38 in (**a**) equilibrium in PBS solution (*n*=8 experiments) and (**b**) tumor disaggregate (**b**) (*n*=3 experiments). The value extrapolated in the curve at the theoretical zero flow rate gives C_{ZFR}.
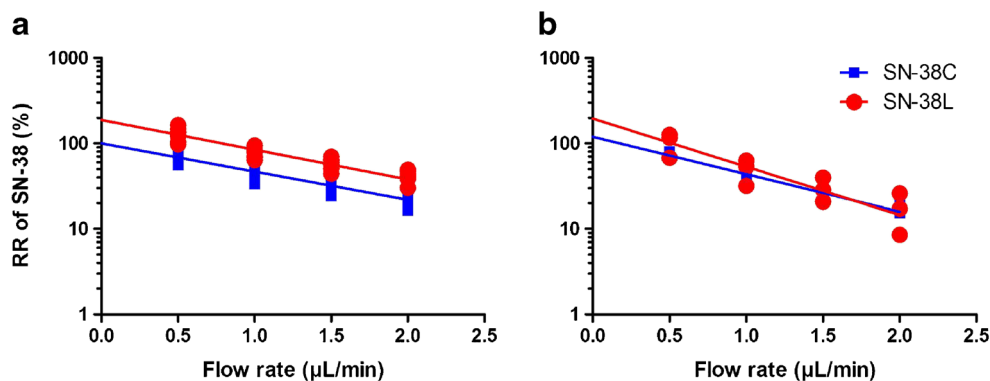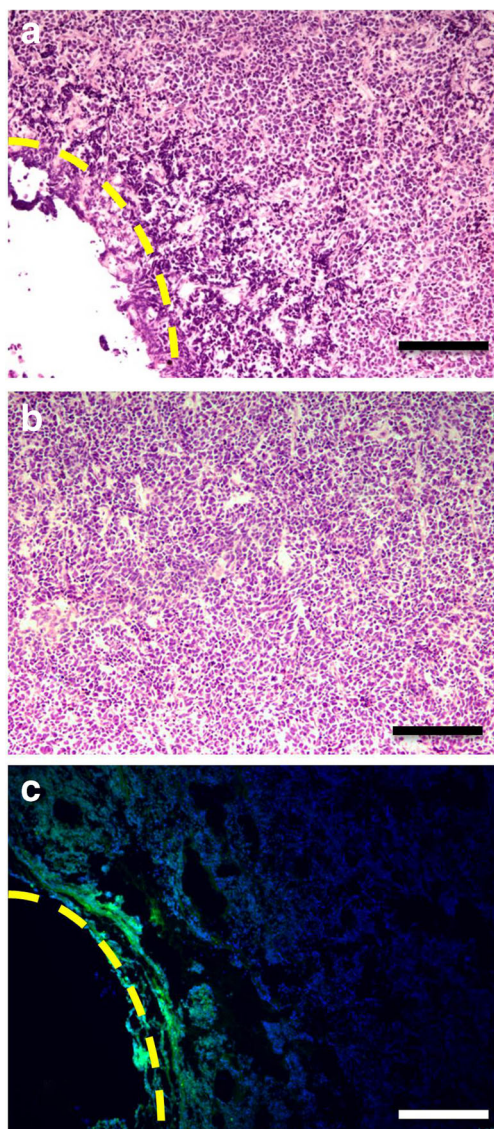
Fig. 5 Histological study of the microdialysis probe track after *in vivo* perfusion of 10% HPBCD-FITC. (**a**) HE-stained section of the probe track. (**b**) HE-stained section of tumor tissue distant from the probe. (**c**) Extravasation of fluorescent HPBCD-FITC from the probe. Cell nuclei were stained with DAPI. *Dashed yellow lines* mark the probe track. Scale bar: 500 μm.

evidences addressing the specific challenges associated with the technique, and they could not distinguish between SN-38 L and SN-38 C forms.

The use of HPBCD as enhancer raises concerns about its interference with the HPLC analytical technique (26). In fact, drug/cyclodextrin complexes are new entities and some of them, especially the complexes with hydrophobic cyclodextrins, display different retention time in HPLC than the free counterparts. This phenomenon takes place when the drug is forming a complex during the chromatographic analysis. Our data showed that the retention times of both SN-38 L and SN-38 C fitted those of cyclodextrin-free SN-38 and suggested that HPBCD complexes underwent decomplexation upon
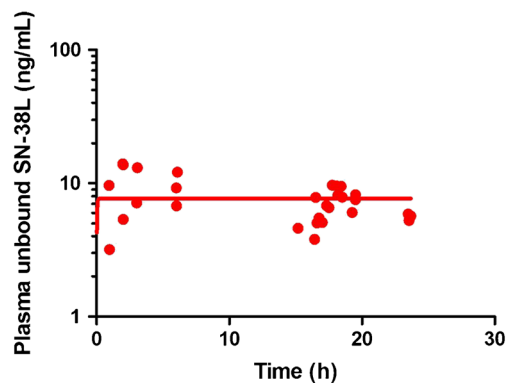
Fig. 6 Plasma concentration of unbound SN-38 L upon infusion with irinotecan-loaded osmotic pumps. Individual data collected during 24 h of study is represented. The *line* represents the best-fitting model obtained after analysis with ADAPT 5 software. Model-fitted $c_{ss,plasma}$ was 7.7 ng/mL.

the addition of methanol and mobile phase for HPLC analysis. At the same time, care should be taken in new applications with other drugs because specific cyclodextrins interfere with columns during drug analysis (33).

The question whether HPBCD interferes with drug distribution within the tumor tissue immediately surrounding the probe is not fully answered by our work. However, our data show limited extravasation of the fluorescent HPBCD derivative from the microdialysis probe, thus it is unlikely that HPBCD modifies drug distribution significantly in the dialyzed tissue. Also, we do not expect that the cyclodextrin will have enough affinity for the drug to alter the distribution in the tumor, because previous work shows that drug delivery from hydrophilic HPBCD-based systems is immediate *in vivo* (34). In a recent microdialysis study in patients using 10% HPBCD in perfusate, tissue metabolite concentrations were within the expected physiological range and tissue blood flow in the probe area was unaltered (26).
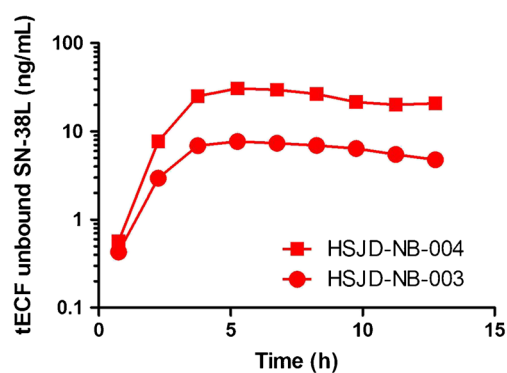
Fig. 7 Representative concentration-time data of unbound SN-38 L in tECF. Data represented come from the analysis of tumor dialysates upon the application of the *f* factor-corrected ZFR method in two animals, bearing the HSJD-NB-003 and HSJD-NB-004 subcutaneous tumor models. Plasma steady state unbound SN-38 L levels achieved for both experiments were 4.2 and 7.0 ng/mL, respectively.

Table I Results of the Combined Microdialysis-Tumor Homogenate Method Experiments for HSJD-NB-003 and HSJD-NB-004 Tumor Models. Data is Represented as mean ± SD (Value in Parenthesis is the Number of Experiments)

Tumor model	$C_{ss,tumor}$ (ng/mL)	$C_{ss,plasma}$ (ng/mL)	$A_{tot,tumor}$ (ng/g tumor)	$V_{tot,blood}$ (µL/g tumor)	$C_{tot,blood}$ (ng/mL)	P_{tumor} [a]	$V_{u,tumor}$ [b] (mL/g tumor)
HSJD-NB-003	7.7 ± 4.6 (3)	4.4 ± 1.9 (11)	25.4 ± 8.5 (10)	26.5 ± 6.6 (4)	21.3 ± 7.4 (4)	2.3 ± 1.4 (3)	3.2 ± 1.1
HSJD-NB-004	10.4 ± 7.6 (4)	6.2 ± 2.2 (12)	76.4 ± 58.7 (12)	15.4 ± 4.5 (3)	19.7 ± 13.7 (2)	1.9 ± 1.2 (4)	7.7 ± 6.0

[a] Calculated from Eq. 9

[b] Calculated from Eq. 1

To calibrate the probe *in vivo* we introduced for the first time the parameter f (Eq. 5) to correct for the extra convection of drug due to the presence of HPBCD in the perfusate. Thus, we preliminarily calculated f in tumor disaggregates *ex vivo*. We acknowledge the difficulty of reproducing intratumor microdialysis conditions *ex vivo*. This issue was addressed by the addition of extracellular volume to the tumor cell suspension and the careful reproduction of the experimental setup (probe, tubing connections, dead volume, flow rate, temperature, tumor cells) used *in vivo*. The validity of the method is strongly supported by the good reproducibility of the parameter f across several independent *in vitro* experiments. Moreover, f values were similar to those obtained in experiments performed under classical *in vitro* conditions (sample in PBS dialysate, unstirred, room temperature). We cannot exclude that our *ex vivo* estimation of f might change upon *in vivo* application. However, previous publications have shown similar *in vitro* and *in vivo* microdialysis recoveries (35, 36).

The hypothesis that suggests that only the free drug (plasma protein unbound) is able to distribute within tissues requires careful consideration in solid tumors. From microdialysis studies in our neuroblastoma models, P_{tumor} values higher than 1 at steady state suggest enhanced drug permeability and retention (EPR effect (37)) in tECF. Such effect was expected from previous microdialysis-based studies detecting enhanced unbound drug distribution in solid tumors (10, 38). Ours is the first report to assess it in neuroblastoma PDX.

From the combination of microdialysis and homogenate data, a $V_{u,tumor}$ value greater than 3 mL/g tumor for both neuroblastoma models suggested that SN-38 L efficiently penetrates tumor cells; compounds that do not enter tumor cells show $V_{u,tumor}$ smaller than 1. The relative contribution of the drug in the tumor vascular compartment ($V_{tot,blood}$ x $C_{tot,blood}$) to $V_{u,tumor}$ was almost negligible in our models. In fact, the elimination of the drug in the vascular compartment (Eq. 1) diminished this parameter in 0.07 and 0.03 mL/g tumor for HSJD-NB-003 and HSJD-NB-004, respectively, which is less than 3% of the $V_{u,tumor}$ value.

The *in vivo* microdialysis technique is challenging and thus, only few studies combined microdialysis and homogenate data to characterize drug distribution in tissues. Two of the most comprehensive works in the field showed the heterogeneity in the colchicine distribution in intra- and extracellular spaces of the hippocampus and other regions of the brain (39) and introduced the parameter of unbound volume of distribution in the brain upon the analysis of gabapentin in brain dialysates and homogenates (9). Such approaches have been further refined to describe the rate and extent of drug delivery to the brain compartments, including the intracellular one (40).

In summary, our detailed *in vitro* and *in vivo* study of the effect of the microdialysis enhancer HPBCD substantiates the reproducible sampling of a very potent and hydrophobic anticancer drug in tECF. We propose the calculation *ex vivo* of an enhancement factor to apply for *in vivo* probe calibration with the ZFR method. Upon the combination of the microdialysis-tumor homogenate method described here, we provide a powerful tool for further distribution studies of lipophilic drugs within solid tumors. In this context, this novel method is being used in our laboratory not only to characterize resistance mechanisms to anticancer agents related to drug distribution parameters in neuroblastoma, Ewing sarcoma and rhabdomyosarcoma PDX models but also to study the effect of novel delivery methods on drug distribution within tumor compartments. These investigations will further contribute to support the relevance of the developed analytical approach and refine it.

ACKNOWLEDGMENTS

REFERENCES

1. Patel KJ, Tredan O, Tannock IF. Distribution of the anticancer drugs doxorubicin, mitoxantrone and topotecan in tumors and normal tissues. Cancer Chemother Pharmacol. 2013;72(1):127–38.

2. Minchinton AI, Tannock IF. Drug penetration in solid tumours. Nat Rev Cancer. 2006;6(8):583–92.

3. Kratz F, Warnecke A. Finding the optimal balance: challenges of improving conventional cancer chemotherapy using suitable combinations with nano-sized drug delivery systems. J Control Release. 2012;164(2):221–35.

4. Provenzano PP, Cuevas C, Chang AE, Goel VK, Von Hoff DD, Hingorani SR. Enzymatic targeting of the stroma ablates physical barriers to treatment of pancreatic ductal adenocarcinoma. Cancer Cell. 2012;21(3):418–29.

5. Fletcher JI, Haber M, Henderson MJ, Norris MD. ABC transporters in cancer: more than just drug efflux pumps. Nat Rev Cancer. 2010;10(2):147–56.

6. Holback H, Yeo Y. Intratumoral drug delivery with nanoparticulate carriers. Pharm Res. 2011;28(8):1819–30.

7. Tuntland T, Ethell B, Kosaka T, Blasco F, Zang RX, Jain M, *et al*. Implementation of pharmacokinetic and pharmacodynamic strategies in early research phases of drug discovery and development at Novartis Institute of Biomedical Research. Front Pharmacol. 2014;5:174.

8. Muller M. Microdialysis in clinical drug delivery studies. Adv Drug Deliv Rev. 2000;45(2–3):255–69.

9. Wang Y, Welty DF. The simultaneous estimation of the influx and efflux blood–brain barrier permeabilities of gabapentin using a microdialysis-pharmacokinetic approach. Pharm Res. 1996;13(3):398–403.

10. Carcaboso AM, Elmeliegy MA, Shen J, Juel SJ, Zhang ZM, Calabrese C, *et al*. Tyrosine kinase inhibitor gefitinib enhances topotecan penetration of gliomas. Cancer Res. 2010;70(11):4499–508.

11. Loos WJ, Zamboni WC, Engels FK, de Bruijn P, Lam MH, de Wit R, *et al*. Pitfalls of the application of microdialysis in clinical oncology: controversial findings with docetaxel. J Pharm Biomed Anal. 2007;45(2):288–94.

12. Whitaker G, Lunte CE. Investigation of microdialysis sampling calibration approaches for lipophilic analytes: doxorubicin. J Pharm Biomed Anal. 2010;53(3):490–6.

13. Lindberger M, Tomson T, Lars S. Microdialysis sampling of carbamazepine, phenytoin and phenobarbital in subcutaneous extracellular fluid and subdural cerebrospinal fluid in humans: an in vitro and in vivo study of adsorption to the sampling device. Pharmacol Toxicol. 2002;91(4):158–65.

14. Khramov AN, Stenken JA. Enhanced microdialysis recovery of some tricyclic antidepressants and structurally related drugs by cyclodextrin-mediated transport. Analyst. 1999;124(7):1027–33.

15. Elmeliegy MA, Carcaboso AM, Tagen M, Bai F, Stewart CF. Role of ATP-binding cassette and solute carrier transporters in Erlotinib CNS penetration and intracellular accumulation. Clin Cancer Res. 2011;17(1):89–99.

16. Müller M, Schmid R, Wagner O, Osten B, Shayganfar H, Eichler HG. In vivo characterization of transdermal drug transport by microdialysis. J Control Release. 1995;37(1–2):49–57.

17. Duo J, Fletcher H, Stenken JA. Natural and synthetic affinity agents as microdialysis sampling mass transport enhancers: current progress and future perspectives. Biosens Bioelectron. 2006;22(3):449–57.

18. Araujo BV, Silva CF, Haas SE, Dalla CT. Microdialysis as a tool to determine free kidney levels of voriconazole in rodents: a model to study the technique feasibility for a moderately lipophilic drug. J Pharm Biomed Anal. 2008;47(4–5):876–81.

19. Warner DL, Burke TG. Simple and versatile high-performance liquid chromatographic method for the simultaneous quantitation of the lactone and carboxylate forms of camptothecin anticancer drugs. J Chromatogr B Biomed Sci Appl. 1997;691(1):161–71.

20. Khramov AN, Stenken JA. Enhanced microdialysis extraction efficiency of ibuprofen in vitro by facilitated transport with beta-cyclodextrin. Anal Chem. 1999;71(7):1257–64.

21. Ao X, Stenken JA. Water-soluble cyclodextrin polymers for enhanced relative recovery of hydrophobic analytes during microdialysis sampling. Analyst. 2003;128(9):1143–9.

22. Menacherry S, Hubert W, Justice Jr JB. In vivo calibration of microdialysis probes for exogenous compounds. Anal Chem. 1992;64(6):577–83.

23. Jacobson I, Sandberg M, Hamberger A. Mass transfer in brain dialysis devices–a new method for the estimation of extracellular amino acids concentration. J Neurosci Methods. 1985;15(3):263–8.

24. D'argenio DZ, Schumitzky A. ADAPT 5 User's guide: pharmacokinetic/ pharmacodynamic systems analysis software. Los Angeles: Biomedical Simulations Resource; 2009.

25. Schuck VJ, Rinas I, Derendorf H. In vitro microdialysis sampling of docetaxel. J Pharm Biomed Anal. 2004;36(4):807–13.

26. May M, Batkai S, Zoerner AA, Tsikas D, Jordan J, Engeli S. Enhanced human tissue microdialysis using hydroxypropyl-ss-cyclodextrin as molecular carrier. PLoS One. 2013;8(4):e60628.

27. Ward KW, Medina SJ, Portelli ST, Mahar Doan KM, Spengler MD, Ben MM, *et al*. Enhancement of in vitro and in vivo microdialysis recovery of SB-265123 using Intralipid and Encapsin as perfusates. Biopharm Drug Dispos. 2003;24(1):17–25.

28. Irie T, Uekama K. Pharmaceutical applications of cyclodextrins. III. Toxicological issues and safety evaluation. J Pharm Sci. 1997;86(2):147–62.

29. Cwiertnia B, Hladon T, Stobiecki M. Stability of diclofenac sodium in the inclusion complex with beta-cyclodextrin in the solid state. J Pharm pharmacol. 1999;51(11):1213–8.

30. Vangara KK, Ali HI, Lu D, Liu JL, Kolluru S, Palakurthi S. SN-38-cyclodextrin complexation and its influence on the solubility, stability, and in vitro anticancer activity against ovarian cancer. AAPS PharmSciTech. 2014;15(2):472–82.

31. Metz MZ, Gutova M, Lacey SF, Abramyants Y, Vo T, Gilchrist M, *et al*. Neural stem cell-mediated delivery of irinotecan-activating carboxylesterases to glioma: implications for clinical use. Stem Cells Transl Med. 2013;2(12):983–92.

32. Dodds HM, Tobin PJ, Stewart CF, Cheshire P, Hanna S, Houghton P, *et al*. The importance of tumor glucuronidase in the activation of irinotecan in a mouse xenograft model. J Pharmacol Exp Ther. 2002;303(2):649–55.

33. Ngim KK, Gu Z, Catalano T. Characterization and resolution of reversed phase HPLC chromatography failure attributed to sulfobutylether-beta-cyclodextrin in a pharmaceutical sample preparation. J Pharm Biomed Anal. 2009;49(3):660–9.

34. Hirayama F, Uekama K. Cyclodextrin-based controlled drug release system. Adv Drug Deliv Rev. 1999;36(1):125–41.

35. Zamboni WC, Houghton PJ, Hulstein JL, Kirstein M, Walsh J, Cheshire PJ, *et al*. Relationship between tumor extracellular fluid exposure to topotecan and tumor response in human neuroblastoma xenograft and cell lines. Cancer Chemother Pharmacol. 1999;43(4):269–76.

36. Dukic S, Kaltenbach ML, Gourdier B, Marty H, Vistelle R. Determination of free extracellular levels of methotrexate by microdialysis in muscle and solid tumor of the rabbit. Pharm Res. 1998;15(1):133–8.

37. Matsumura Y, Maeda H. A new concept for macromolecular therapeutics in cancer chemotherapy: mechanism of tumoritropic accumulation of proteins and the antitumor agent smancs. Cancer Res. 1986;46(12 Pt 1):6387–92.

38. Zhou Q, Lv H, Mazloom AR, Xu H, Ma'ayan A, Gallo JM. Activation of alternate prosurvival pathways accounts for acquired sunitinib resistance in U87MG glioma xenografts. J Pharmacol Exp Ther. 2012;343(2):509–19.

39. Evrard PA, Ragusi C, Boschi G, Verbeeck RK, Scherrmann JM. Simultaneous microdialysis in brain and blood of the mouse: extracellular and intracellular brain colchicine disposition. Brain Res. 1998;786(1–2):122–7.

40. Hammarlund-Udenaes M, Friden M, Syvanen S, Gupta A. On the rate and extent of drug delivery to the brain. Pharm Res. 2008;25(8): 1737–50.